through the solution for 5 s. Ethanol (20 mL) was then added, and the dichloromethane was removed at reduced pressure to give the product as white crystals (45 mg, 98%).

$[Ir(CH_3CN)(C_2F_4)(CO)(PPh_3)_2]ClO_4$. $[Ir(CH_3CN)(CO)(PPh_3)_2]ClO_4$ (500 mg, 0.57 mmol) was dissolved in benzene (30 mL) and stirred under tetrafluoroethylene pressure (500 kPa) in a Fischer–Porter bottle (volume 300 mL) for 3 h. The tetrafluoroethylene was then vented, and the benzene was removed in vacuo. The residue was recrystallized from dichloromethane and ethanol to give the product as white crystals (544 mg, 97%), mp 185–187 °C. Anal. Calcd for $C_{41}H_{33}ClF_4IrO_5NP_2$: C, 49.98; H, 3.38; N, 1.42; F, 7.71. Found: C, 50.31; H, 3.60; F, 6.97. IR (Nujol, cm^{-1}): ν(CO) 2068; ν(CF) 1139, 1072, 801; ν(CN) 2335. ^1H NMR ($CDCl_3$, ppm): 2.06 (s, 3 H, CH_3CN). ^{31}P NMR ($CDCl_3$, ppm): −7.04 (m). ^{19}F ($CDCl_3$, ppm): −113.3 (ddm, $^2J_{FF}$ = 165 Hz, $^3J_{FF}$ = 39 Hz, C_2F_4 (F trans to CO)), −119.4 (dm, $^2J_{FF}$ = 165 Hz, C_2F_4 (F trans to CH_3CN)). ^{13}C NMR ($CDCl_3$, ppm): 161.5 (m, CO), 174 (m, CH_3CN), 2.8 (s, CH_3CN), 93.1 (ddd, $^1J_{FC}$ = 328.0 Hz, $^1J_{FC}$ = 339.1 Hz, $^2J_{CP}$ = 87.6 Hz, C_2F_4), 128.9 (d, $^1J_{CP}$ = 46.2 Hz, ipso PPh_3), 133.0 (d, $^2J_{CP}$ = 11.2 Hz, ortho PPh_3), 129.4 (d, $^3J_{CP}$ = 10.6 Hz, meta PPh_3), 132.0 (d, $^4J_{CP}$ = 1.9 Hz, para PPh_3).

$Ir(CF_2CF_2H)(CO)(PPh_3)_2$. $Ir(CF_2CF_2H)(C_2H_4)(CO)(PPh_3)_2$ (200 mg, 0.2 mmol) was heated, at 90 °C, under dynamic vacuum for 2 h. During this time the color changed from white to yellow. The complex was characterized spectroscopically. IR (Nujol, cm^{-1}): ν(CO) 1964; ν(CF) 1166, 1150, 1087, 1019, 976, 968, 935, 776. ^1H NMR ($CDCl_3$, ppm): 4.88 (tt, 1 H, $^2J_{FH}$ = 54.8 Hz, $^3J_{FH}$ = 6.7 Hz, CF_2CF_2H). ^{31}P NMR ($CDCl_3$, ppm): 4.04 (t, $^3J_{PF}$ = 15.3 Hz).

***cis*-$IrCl_2(CF_2CF_2H)(CO)(PPh_3)_2$.** $Ir(CF_2CF_2H)(CO)(PPh_3)_2$ (100 mg, 0.1 mmol) was dissolved in dichloromethane (10 mL). Iododichlorobenzene (0.1 mmol) was added and the solution stirred for 5 min, during which time the yellow color faded. Ethanol (20 mL) was added, and the dichloromethane was removed at reduced pressure. The product was isolated as colorless crystals (62 mg, 77%), mp 195–198 °C. Anal. Calcd for $C_{39}H_{31}Cl_2F_4IrOP_2$: C, 51.10; H, 3.40; F, 8.29. Found: C, 51.33; H, 3.59; F, 8.08. IR (Nujol, cm^{-1}): ν(CO) 2073; ν(CF) 1162, 1094, 999, 907, 846. ^1H NMR ($CDCl_3$, ppm): 4.92 (tt, 1 H, $^2J_{FH}$ = 53.7 Hz, $^3J_{FH}$ = 7.21 Hz, CF_2CF_2H). ^{31}P NMR ($CDCl_3$, ppm): −21.48 (t, $^3J_{PF}$ = 20.5 Hz).

X-ray Collection and Refinement. Crystals suitable for data collection were grown from a dichloromethane/ethanol solution. The cell parameters were determined by a least-squares refinement of 25 accurately centered reflections. Crystal stability was monitored by recording three check reflections every 100 reflections, and no significant variations were observed. The data were corrected for Lorentz and polarization effects, and an empirical absorption correction was applied, on the basis of the ψ-scan data and the crystal dimensions. A Patterson synthesis revealed the position of the heavy atom, and the remaining non-hydrogen atoms were located with use of Fourier maps. Atomic scattering factors were for neutral atoms. Anisotropic thermal parameters were assigned to all but the atoms of the phenyl rings. The structure solution and refinement utilized SHELX-76.[11] Details of the crystal data and intensity data collection parameters are summarized along with atom positions in Tables II and III.

Acknowledgment. We are grateful to the University of Canterbury Chemistry Department X-ray crystallographic section for collecting the data for $Ir(CF_2CF_2H)(CO)_2(PPh_3)_2$ and to Dr. C. E. F. Rickard for helpful discussions.

Supplementary Material Available: Thermal factors (Tables IV and V), bond lengths (Table VI), and bond angles (Table VII) (5 pages); a listing of the structure factors (11 pages). Ordering information is given on any current masthead page.

(11) Sheldrick, G. M. SHELX-76; University Chemical Laboratory: Cambridge, England, 1976.

(12) Lewis, E. E.; Naylor, M. A. *J. Am. Chem. Soc.* **1947**, *69*, 1968. van Gaal, H. L. M.; van der Ent, A. *Inorg. Chim. Acta* **1973**, *7*, 653. Bonnet, J. J.; Mathieu, R.; Poilblanc, R.; Ibers, J. A. *J. Am. Chem. Soc.* **1979**, *101*, 7487.

Cooperative Activation of CO by Early/Late Heterobimetallics: Reactions of $[Cp_2M(\mu\text{-}PR_2)]_2$ (M = Ti, Zr) with $[CpMo(CO)_3]_2$

David G. Dick and Douglas W. Stephan*

Department of Chemistry and Biochemistry, University of Windsor, Windsor, Ontario, Canada N9B 3P4

Received December 6, 1989

The reactions of the Ti(III) and Zr(III) species $[Cp_2M(\mu\text{-}PEt_2)]_2$ with $[CpMo(CO)_3]_2$ have been studied. In the Zr case, the reaction proceeds with reduction of the Mo–Mo bond and concurrent oxidation of the Zr(III) center to Zr(IV). The product is formulated as $Cp_2Zr(\mu\text{-}PEt_2)(\mu\text{-}\eta^1,\eta^2\text{-}OC)Mo(CO)Cp$ (**1**). Compound **1** crystallizes in the monoclinic space group $P2_1/c$ with a = 14.644 (2) Å, b = 9.795 (2) Å, c = 14.667 (3) Å, β = 104.27 (1)°, Z = 4, and V = 2039 (1) Å^3. The reaction of the Ti(III) phosphide species with $[CpMo(CO)_3]_2$ proceeds via an alternate pathway. Reduction of the Mo–Mo bond occurs with oxidation of the phosphide ligand on Ti, affording the complex $Cp_2Ti(THF)(\mu\text{-}\eta^1,\eta^1\text{-}OC)Mo(CO)_2Cp$ (**2**) and P_2Et_4. The Ti(III)/Mo(0) complex **2** crystallizes in the triclinic space group $P\bar{1}$ with a = 16.320 (4) Å, b = 7.907 (2) Å, c = 10.882 (3) Å, α = 115.39 (1)°, β = 82.99 (2)°, γ = 124.66 (2)°, Z = 2, and V = 1029 (1) Å^3. The spectral and structural characterizations of complexes **1** and **2** are presented. The differing modes of CO activation in species **1** and **2** are described, and the implications regarding heterobimetallic activation of CO are discussed.

Introduction

Recently, numerous studies have described complexes containing both early, oxophilic and late, electron-rich metals.[1] Interest in such heterobimetallic complexes has arisen, as such metal pairings combine the Lewis acidity of the early metals and the known ability of late-metal centers to activate hydrogen, thus offering the potential of carbon oxide activation and reduction. A number of synthetic routes to homogeneous early/late heterobimetallic complexes have been reported.[1] Although a number of complexes have been described where the constituent metals are linked by metal–metal bonds,

(1) The subject of early/late heterobimetallics has been recently reviewed: Stephan, D. W. *Coord. Chem. Rev.* **1989**, *95*, 41.

0276-7333/90/2309-1910$02.50/0

Scheme I

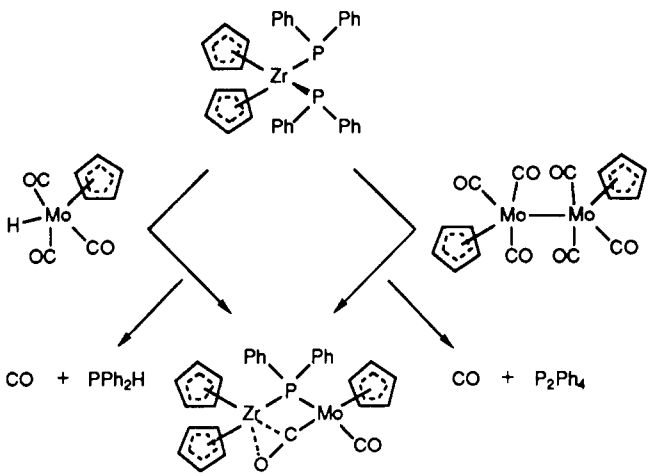

bridging hyrides, carbonyls, or other carbon-based fragments, the majority of known heterobimetallic complexes contain bridging or linking ligands.[1] A variety of systems containing pendant chelate ligands have been described.[2] Such compounds are unique and interesting, but only in specific cases will the nature of the ligands permit interactions of the disparate metal centers with a common substrate. In contrast, single-atom-bridging ligands such as thiolates or phosphides ensure that the early- and late-metal centers are in closer proximity. We and others have described a number of such early/late heterobimetallic complexes in which two thiolate or phosphide ligands link the constituent metals.[3] While such systems are of interest synthetically, the known systems did not offer a vacant coordination site on the early metal and thus precluded the Lewis acid activation of a late-metal-bound carbonyl ligand. In a recent report,[3c] we described monophosphido-bridged species of the form $Cp_2Zr(\mu\text{-}PPh_2)(\mu\text{-}\eta^1,\eta^2\text{-}OC)M(CO)Cp$ (M = Mo, W), in which the two metal centers are held in close proximity by the bridging phosphide, affording the Lewis acid activation of the carbonyl ligand bound to Mo. Synthesis of these complexes was achieved by two routes. The reaction of $Cp_2Zr(PPh_2)_2$ with $[CpM(CO)_3]_2$ affords reduction of the M–M bond with concurrent oxidation of one of the phosphide ligands on Zr. Alternatively, reaction of $Cp_2Zr(PPh_2)_2$ with $CpM(CO)_3H$ yields the monophosphido-bridged heterobimetallic and PPh_2H (Scheme I).

In an effort to develop new synthetic methods for the preparation of related heterobimetallic systems, we have examined the reactions of Ti(III) and Zr(III) phosphides with $[CpMo(CO)_3]_2$. In the case of Zr, reduction of the Mo–Mo bond occurs with concomitant oxidation of Zr(III) to Zr(IV). This reaction provides an alternative synthetic route to monophosphido-bridged heterobimetallics in which a carbonyl moiety is cooperatively activated by interaction with both the early- and late-metal centers. In contrast, the analogous reaction involving the Ti(III) phosphide proceeds with reduction of the Mo–Mo bond and oxidation of the phosphide ligand. The resulting heterobimetallic species incorporates Ti(III) and Mo(0) metal centers that are linked only by a bridging CO moiety. The nature and structure of the products of these reactions have been characterized by spectroscopy and crystallography. These studies are presented herein, and the implications of these results regarding heterobimetallic activation of CO are considered.

Experimental Section

General Data. All preparations were done under an atmosphere of dry, O_2-free N_2 in a Vacuum Atmospheres inert-atmosphere glovebox. The atmosphere quality is maintained by employing a constant-circulation 5-cfm purifier containing the Chemical Dynamics Corp. catalyst R3-11. Solvents were reagent grade, distilled from the appropriate drying agents under N_2 and degassed by the freeze–thaw method at least three times prior to use. ^1H and $^{13}C\{^1H\}$ NMR spectra were recorded on a Bruker AC-300 spectrometer operating at 300 and 75 MHz, respectively. Trace amounts of protonated solvents were used as references, and chemical shifts are reported relative to $SiMe_4$. $^{31}P\{^1H\}$ NMR spectra were recorded on a Bruker AC-200 NMR spectrometer operating at 81 MHz and are reported relative to 85% H_3PO_4 as an external reference. Infrared absorption data were recorded on a Nicolet 5DX Fourier transform IR spectrometer. EPR spectra were recorded on a Varian E-12 EPR spectrometer, with DPPH as the spectral reference. Combustion analyses were performed by Galbraith Laboratories Inc., Knoxville, TN, and Schwartzkopf Microanalytical Laboratories, Woodside, NY. Typical synthetic routes to complexes of the form $[Cp_2M(\mu\text{-}PR_2)]_2$ (M = Ti, Zr) have been previously described in the literature.[4] Cp_2ZrCl_2 and $[CpMo(CO)_3]_2$ were purchased from the Aldrich Chemical Co. PEt_2H was purchased from the Strem Chemical Co.

Synthesis of $LiPEt_2$. To a cooled hexane solution (60 mL, 0 °C) containing PEt_2H (5.7 g, 63 mmol) was added 26 mL (65 mmol) of 2.5 M *n*-BuLi in hexane. The solution was gradually warmed to 35 °C. A white precipitate formed rapidly, and the solution was allowed to stand for 2 h. The product was isolated by filtration and dried in vacuo (4.85 g, 50 mmol, 80% yield). $^{31}P\{^1H\}$ NMR (THF): −54.6 ppm. The ^1H-coupled ^{31}P NMR spectra showed no evidence of P–H coupling.

Synthesis of $Cp_2Zr(\mu\text{-}PEt_2)(\mu\text{-}\eta^1,\eta^2\text{-}OC)Mo(CO)Cp$ (1). (i) To a THF solution of Cp_2ZrCl_2 (0.080 g, 0.27 mmol) was added a THF solution containing $LiPEt_2$ (0.054 g, 0.56 mmol). The resulting red solution was added to a THF solution of $[CpMo(CO)_3]_2$ (0.067 g, 0.14 mmol). Vapor diffusion of hexane into the THF solution yielded yellow crystals of 1 (0.101 g, 0.19 mmol, 70% yield).

(ii) To a THF solution of $[Cp_2Zr(\mu\text{-}PEt_2)]_2$ (0.016 g, 0.026 mmol) was added a THF solution of $[CpMo(CO)_3]_2$ (0.013 g, 0.026 mmol). The solution became yellow after being stirred for 15 min. $^{31}P\{^1H\}$ NMR studies showed the exclusive formation of 1 in apparently quantitative yield. A yellow solid was isolated by addition of hexane and filtration (0.019 g, 0.036 mmol, 70% yield). Anal. Calcd for $C_{21}H_{25}MoO_2PZr$: C, 47.81; H, 4.78. Found: C, 47.20; H, 4.40. ^1H NMR (C_6D_6, δ, ppm): 5.43 (d, 5 H, $|J_{P\text{-}H}|$ = 1.1 Hz), 5.18 (d, 5 H, $|J_{P\text{-}H}|$ = 1.1 Hz), 4.99 (d, 5 H, $|J_{P\text{-}H}|$ = 0.5 Hz), 2.32 (m, 2 H), 2.14 (m, 2 H), 1.28 (d of t, 3 H, $|J_{P\text{-}H}|$ = 14.4 Hz, $|J_{H\text{-}H}|$ = 7.3 Hz), 1.11 (d of t, 3 H, $|J_{P\text{-}H}|$ = 13.4 Hz, $|J_{H\text{-}H}|$ = 6.9 Hz). $^{31}P\{^1H\}$ NMR (THF, δ, ppm): 156.4 (s). IR (THF, cm^{-1}): 1848, 1567.

Synthesis of $Cp_2Ti(THF)(\mu\text{-}OC)Mo(CO)_2Cp$ (2). (i) To a THF solution of $[Cp_2Ti(\mu\text{-}PPh_2)]_2$ (0.015 g, 0.020 mmol) was added a THF solution of $[CpMo(CO)_3]_2$ (0.010 g, 0.0020 mmol). The solution became green after 15 min and was allowed to stand for 1 h. The $^{31}P\{^1H\}$ NMR spectrum showed the formation of P_2Ph_4 (δ = −15.5 ppm). Hexane was carefully layered on this solution.

(2) Pendant chelate linked heterobimetallic systems have been reviewed in ref 1. Recent papers describing such systems include: (a) Anderson, G. K.; Lin, M. *Organometallics* **1988**, *7*, 2285. (b) Ferguson, G. S.; Wolczanski, P. T.; Parkanyi, L.; Zonnvylle, M. C. *Organometallics* **1988**, *7*, 1967.

(3) Phosphido- and thiolato-bridged heterobimetallics have been described in ref 1. Recent papers describing such systems include: (a) Wark, T. A.; Stephan, D. W. *Organometallics* **1989**, *8*, 2836. (b) Wark, T. A.; Stephan, D. W. *Inorg. Chem.*, in press. (c) Zheng, P. Y.; Nadasdi, T. T.; Stephan, D. W. *Organometallics* **1989**, *8*, 1393. (d) Darensbourg, M. Y.; Silva, R.; Reibenspies, J.; Prout, C. K. *Organometallics* **1989**, *8*, 1315.

(4) (a) Issleib, K.; Hackert, H. *Z. Naturforsch.* **1966**, *21B*, 519. (b) Kenworthy, J. G.; Myatt, J.; Todd, P. F. *J. Chem. Soc. B* **1970**, 792. (c) Payne, R.; Hachgenei, J.; Fritz, G.; Fenske, D. *Z. Naturforsch.* **1986**, *41B*, 1535. (d) Wade, S. R.; Wallbridge, G. H.; Willey, G. R. *J. Chem. Soc., Dalton Trans.* **1983**, 2555.

Table I. Crystallographic Parameters

	1	2
formula	$C_{21}H_{25}MoO_2PZr$	$C_{22}H_{23}MoO_4Ti$
cryst color, form	yellow blocks	green plates
a, Å	14.644 (2)	16.320 (4)
b, Å	9.795 (2)	7.907 (2)
c, Å	14.667 (3)	10.882 (3)
α, deg		115.39 (2)
β, deg	104.27 (1)	82.99 (2)
γ, deg		124.66 (2)
cryst syst	monoclinic	triclinic
space group	$P2_1/c$	$P\bar{1}$
V, Å^3	2038.8 (6)	1029.4 (5)
calcd density, g cm^{-3}	1.71	1.73
Z	4	2
cryst dimens, mm	0.42 × 0.57 × 0.54	0.65 × 0.38 × 0.52
abs coeff, μ, cm^{-1}	10.92	7.13
radiation λ, Å	Mo Kα 0.710 69)	Mo Kα (0.710 69)
temp, °C	24	24
scan speed, deg min^{-1}	2.0–10.0 ($\theta/2\theta$)	2.0–10.0 ($\theta/2\theta$)
scan range, deg	1.0 below Kα_1, 1.0 above Kα_2	1.0 below Kα_1, 1.0 above Kα_2
bkgd/scan time ratio	0.5	0.5
no. of data collected	3224	2691
2θ range, deg	4.5–45.0	4.5–45.0
index range	$\pm h,+k,+l$	$\pm h,\pm k,+l$
no. of unique data with $F_o^2 > 3\sigma(F_o^2)$	2338	2252
variable	236	253
R, %	2.08	2.70
R_w, %	2.59	3.37
largest Δ/σ in final least-squares cycle	0.004	0.005
max residual, e Å^{-3}	0.35	0.35
atom associated	Mo	Ti

The solution was allowed to stand undisturbed while the solvents slowly diffused together. This afforded green crystals of **2**.

(ii) To a THF solution of $[Cp_2Ti(\mu\text{-}PEt_2)]_2$ (0.010 g, 0.018 mmol) was added a THF solution of $[CpMo(CO)_3]_2$ (0.009 g, 0.018 mmol). The solution immediately became green and was allowed to stand for 1 h. The $^{31}P\{^1H\}$ NMR spectrum showed the formation of P_2Et_4 (δ = −32.6 ppm). Crystalline **2** was obtained on standing. The crystalline product was isolated by filtration. Diffusion of hexane into the mother liquor afforded more product (yield 0.009 g, 0.018 mol, 50%). EPR (THF): g = 1.977, $\langle a \rangle$ = 12 G. IR (THF, cm^{-1}): 1920, 1829, 1652.

Attempted Reactions of 1. Small-scale reactions of **1** were attempted with MeLi and $LiBHEt_3$. These reactions were performed in a similar fashion, and thus only one example procedure is given. To a THF solution of **1** was added a THF solution of $LiBHEt_3$ (2.2 equiv). The reaction mixture was allowed to stand for 4 h and the progress of the reaction monitored by $^{31}P\{^1H\}$ NMR spectroscopy.

X-ray Data Collection and Reduction. Diffraction experiments were performed on a four-circle Syntex $P2_1$ diffractometer with graphite-monochromatized Mo Kα radiation. The initial orientation matrix was obtained from 15 machine-centered reflections selected from rotation photographs. These data were used to determine the crystal system. Partial rotation photographs around each axis were consistent with monoclinic and triclinic crystal systems for **1** and **2**, respectively. Ultimately, 30 and 35 reflections ($20° < 2\theta < 25°$) were used to obtain the final lattice parameters and the orientation matrices. Machine parameters, crystal data, and data collection parameters are summarized in Table I. The observed extinctions were consistent with the space group $P2_1/c$ for **1**. The symmetry of the cell for **2** was consistent with the space group $P1$ or $P\bar{1}$. Successful refinement of the structure of **2** confirmed the space group as $P\bar{1}$. The data were collected ($4.5° < 2\theta < 45.0°$), and three standard reflections were recorded every 197 reflections. The intensities of the standards showed no statistically significant change over the duration of the data collection. The data were processed with use of the SHELX-76 program package on the computing facilities at the University of Windsor. The reflections with $F_o^2 > 3\sigma F_o^2$ were used in the refinement. No absorption corrections were applied to the data, as in both cases, the μ values are small and the crystal dimensions are not markedly anisotropic.

Scheme II

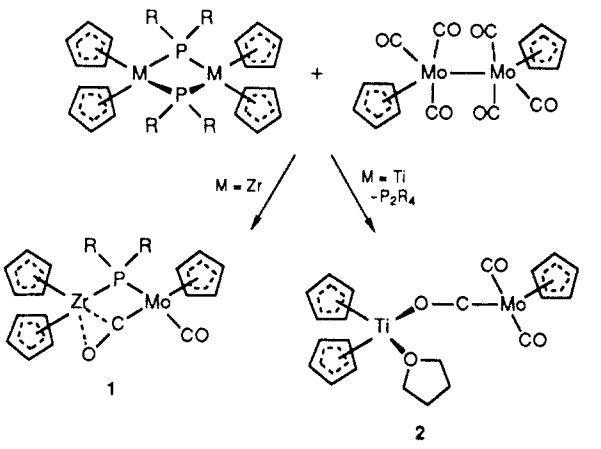

Structure Solution and Refinement. Non-hydrogen atomic scattering factors were taken from the literature tabulations.[5] The metal atom positions were determined by direct methods with use of SHELX-86. The remaining non-hydrogen atoms were located from successive difference Fourier map calculations. The refinements were carried out by using full-matrix least-squares techniques on F, minimizing the function $w(|F_o| - |F_c|)^2$, where the weight, w, is defined as $4F_o^2/2\sigma(F_o^2)$ and F_o and F_c are the observed and calculated structure factor amplitudes. In the final cycles of refinement all the non-hydrogen atoms were assigned anisotropic temeprature factors. Hydrogen atom positions were calculated and allowed to ride on the carbon to which they are bonded, assuming a C–H bond length of 0.95 Å. Hydrogen atom temperature factors were fixed at 1.10 times the isotropic temperature factor of the carbon atom to which they are bonded. In all cases the hydrogen atom contributions were calculated but not refined. The final values of R and R_w are given in Table I. The maximum Δ/σ on any of the parameters in the final cycles of the refinement and the location of the largest peaks in the final difference Fourier map calculation are also given in Table I. The residual electron densities were of no chemical significance. The following data are tabulated: positional parameters (Table II) and selected bond distances and angles (Table III). Thermal parameters (Table S1), hydrogen atom parameters (Table S2), bond distances and angles associated with the cyclopentadienyl groups (Table S3), and values of $10F_o$ and $10F_c$ (Table S4) have been deposited as supplementary material.

Results and Discussion

The reaction of $LiPEt_2$ with Cp_2ZrCl_2 is known to give the Zr(III) dimer $[Cp_2Zr(\mu\text{-}PEt_2)]_2$.[4a] Reaction of this species in THF with $[CpMo(CO)_3]_2$ led to a gradual color change from deep red to red-yellow over a period of 15 min. Monitoring of the reaction by $^{31}P\{^1H\}$ NMR spectroscopy showed a peak at 156 ppm attributable to the new species **1** (Scheme II). This new species can also be generated by reaction of isolated $[Cp_2Zr(\mu\text{-}PEt_2)]_2$ with $[CpMo(CO)_3]_2$ in THF. The use of purified $[Cp_2Zr(\mu\text{-}PEt_2)]_2$ results in a clean yellow solution upon reaction, which yields the yellow crystalline product **1** following addition of hexane. The ^{31}P chemical shift of **1** is similar to that seen for $Cp_2Zr(PEt_2)_2$, suggesting the presence of a Zr(IV)–phosphide fragment.[6] The NMR spectra show ^1H resonances at 5.43, 5.18, and 4.99 ppm and $^{13}C\{^1H\}$ resonances at 106.5,

(5) (a) Cromer, D. T.; Mann, J. B. *Acta Crystallogr., Sect. A: Crystl. Phys., Diffr., Theor. Gen. Crystallogr.* **1968**, *A24*, 324. (b) Cromer, D. T.; Mann, J. B. *Acta Crystallogr., Sect. A: Cryst. Phys., Diffr., Theor. Gen. Crystallogr.* **1968**, *A24*, 390. (c) Cromer, D. T.; Waber, J. T. *International Tables for X-ray Crystallography*; Kynoch Press: Birmingham, England, 1974.

(6) Baker, R. T.; Whitney, J. F.; Wreford, S. S. *Organometallics* **1983**, *2*, 1049.

Table II. Positional Parameters ($\times 10^4$)

atom	x	y	z	atom	x	y	z
			Molecule 1				
Mo	2543 (0)	282 (0)	4597 (0)	Zr	3389 (0)	−1914 (0)	3367 (0)
P	1740 (1)	−678 (1)	3107 (1)	O1	4350 (1)	−1469 (2)	4824 (1)
O2	1575 (2)	−1836 (3)	5597 (2)	C1	3652 (2)	−773 (3)	4816 (2)
C2	1947 (3)	−1073 (4)	5207 (2)	C3	1311 (3)	546 (3)	2138 (2)
C4	797 (3)	−54 (4)	1193 (3)	C5	648 (2)	−1657 (4)	3052 (3)
C6	−138 (3)	−796 (5)	3244 (4)	C11	2594 (3)	−3850 (3)	3993 (3)
C12	2350 (3)	−3969 (3)	3008 (3)	C13	3159 (3)	−4294 (3)	2721 (2)
C14	3908 (3)	−4367 (3)	3524 (2)	C15	3558 (3)	−4110 (3)	4311 (2)
C21	1749 (3)	2407 (4)	4250 (4)	C22	2627 (5)	2566 (4)	4128 (3)
C23	3257 (4)	2372 (4)	5011 (5)	C24	2722 (6)	2086 (5)	5635 (3)
C25	1803 (5)	2117 (5)	5157 (5)	C31	3863 (3)	191 (4)	2612 (3)
C32	3400 (3)	−641 (5)	1876 (2)	C33	3930 (3)	−1791 (4)	1878 (2)
C34	4727 (3)	−1700 (4)	2609 (3)	C35	4690 (3)	−468 (4)	3060 (2)
			Molecule 2				
Mo	6730 (0)	4848 (1)	6952 (0)	Ti	7851 (1)	5377 (1)	2593 (1)
O1	7911 (3)	5474 (6)	4566 (3)	O2	8789 (3)	8862 (7)	8886 (4)
O3	7032 (3)	1159 (6)	6613 (4)	O4	9229 (2)	5543 (5)	2739 (3)
C1	7445 (3)	5189 (7)	5490 (4)	C2	8012 (3)	7309 (8)	8162 (5)
C3	6949 (3)	2590 (7)	6759 (4)	C4	9413 (4)	4561 (9)	3447 (5)
C5	10381 (4)	4840 (9)	3095 (5)	C6	10444 (5)	4913 (13)	1761 (6)
C7	9945 (4)	6010 (11)	1800 (6)	C11	4944 (3)	2416 (8)	6585 (5)
C12	5261 (3)	3639 (8)	7998 (5)	C13	5731 (4)	5914 (8)	8374 (6)
C14	5713 (4)	6173 (10)	7163 (8)	C15	5229 (4)	3974 (10)	6071 (6)
C21	7361 (5)	1762 (9)	794 (8)	C22	6988 (5)	2626 (11)	327 (6)
C23	6291 (4)	2744 (9)	1103 (7)	C24	6218 (4)	2037 (9)	2102 (6)
C25	6892 (4)	1441 (8)	1923 (8)	C31	7811 (5)	7742 (10)	1867 (7)
C32	7442 (6)	7997 (13)	3090 (12)	C33	8215 (8)	9012 (11)	4107 (8)
C34	9067 (5)	9370 (8)	3479 (7)	C35	8801 (4)	8568 (8)	2105 (6)

105.7, and 88.0 ppm, which are attributable to three inequivalent cyclopentadienyl groups. In the ^1H NMR spectrum coupling of the cyclopentadienyl protons to a single phosphorus nucleus is evident. The two downfield resonances are assigned to Zr-bound cyclopentadienyl groups, while the upfield resonance arises from a cyclopentadienyl ligand on Mo. ^1H NMR data for **1** also show multiplets centered at 2.32, 2.14, 1.28, and 1.19 ppm attributable to the inequivalent methylene and methyl moieties of the ethyl substituents on phosphorus. IR absorptions at 1848 and 1567 cm^{-1} are assigned to terminal and bridging carbonyl groups, respectively. These spectroscopic data, in addition to combustion analyses, are consistent with the formulation of **1** as $Cp_2Zr(\mu\text{-}PEt_2)(\mu\text{-}OC)Mo(CO)Cp$. The similarity of the IR stretching frequencies observed for **1** to those of the known compound $Cp_2Zr(\mu\text{-}PPh_2)(\mu\text{-}\eta^1,\eta^2\text{-}OC)Mo(CO)Cp$[3c] suggests the presence of an η^1,η^2-carbonyl fragment. This was confirmed by an X-ray crystallographic study (vide infra). Resonances in the ^1H, ^{13}C, and $^{31}P\{^1H\}$ NMR spectra of **1** are shifted upfield relative to the corresponding resonances in $Cp_2Zr(\mu\text{-}PPh_2)(\mu\text{-}\eta^1,\eta^2\text{-}OC)Mo(CO)Cp$, consistent with the greater electron donor ability of PEt_2 versus that of PPh_2. Similarly, the slightly lower CO stretching frequencies observed for **1** are consistent with greater electron density at Mo.

Studies of $Cp_2Zr(\mu\text{-}PPh_2)(\mu\text{-}\eta^1,\eta^2\text{-}OC)Mo(CO)Cp$[3c] showed that carbonyl site exchange did not occur in solution within the temperature range available in various solvents. Similarly, the lack of reactivity further sugested the lack of lability of the η^1,η^2-carbonyl ligand. It was suggested that the steric demands of the cyclopentadienyl ligands and the bridging diphenylphosphido group precluded reaction at the η^1,η^2-carbonyl moiety. Attempts to effect reaction of **1** were also undertaken. For example, the $^{31}P\{^1H\}$ NMR spectrum of a mixture of **1** with excess $LiBEt_3H$ showed no evidence of reaction. Although the steric demands of the bridging phosphide group are reduced by the inclusion of the PEt_2 moiety in **1**, this perturbation does not afford reactivity at the η^1,η^2-carbonyl. This suggests that it is the steric constraints of the cyclopentadienyl groups on Zr and Mo that inhibit attack of the carbonyl. This is consistent with the similar lack of reactivity observed for $Cp_2Zr(\eta^2\text{-}OCMe)(\mu\text{-}\eta^1,\eta^2\text{-}OC)Mo(CO)Cp$,[7] $Cp_2Nb(\mu\text{-}CO)(\mu\text{-}\eta^1,\eta^2\text{-}OC)Mo(CO)Cp$,[8] and $Cp_2Ti(\mu\text{-}CR)(\mu\text{-}\eta^1,\eta^2\text{-}OC)W(CO)Cp$.[9]

In a manner similar to that used to prepare **1**, the Ti(III) species $[Cp_2Ti(\mu\text{-}PEt_2)]_2$[4c] was reacted with $[CpMo(CO)_3]_2$. The solution became green on stirring. $^{31}P\{^1H\}$ NMR spectroscopy revealed the formation of P_2Et_4. No resonance attributable to a Ti analogue of **1** was observed. Addition of hexane to the reaction mixture afforded the green crystalline product **2** (Scheme II). The IR spectrum of this product displays carbonyl stretching frequencies at 1920, 1829, and 1652 cm^{-1}. The EPR spectrum showed a single resonance at $g = 1.977$. Hyperfine couplings to ^{45}Ti and ^{47}Ti are consistent with the presence of a Ti(III) center in the product **2**. An X-ray structural study determined that **2** is formulated as $Cp_2Ti(THF)(\mu\text{-}\eta^1,\eta^1\text{-}OC)Mo(CO)_2Cp$ (vide infra). Compound **2** was also prepared by the similar reaction of $[Cp_2Ti(\mu\text{-}PPh_2)]_2$ and $[CpMo(CO)_3]_2$. The byproduct in this case is of course P_2Ph_4. Isolation of the green crystalline product **2** and removal of the diphosphine are readily accomplished by washing the product with benzene. An earlier communication reported the synthesis and structure of **2** from the reaction of $Cp_2Ti(CO)_2$ and $CpMo(CO)_2{\equiv}Mo(CO)_2Cp$.[10]

(7) (a) Longato, B.; Norton, J. R.; Huffman, J. C.; Marsella, J. A.; Caulton, K. G. *J. Am. Chem. Soc.* **1981**, *103*, 209. (b) Huffman, J. C.; Marsella, J. A.; Caulton, K. G. *J. Am. Chem. Soc.* **1982**, *104*, 6360.

(8) Pasynskii, A. A.; Skripkin, Y. V.; Kalinnikov, V. T.; Porai-Koshits, M. A.; Antsyshkina, A. S.; Sadikov, G. G.; Ostrikova, V. N. *J. Organomet. Chem.* **1977**, *141*, 313.

(9) Barr, R. D.; Green, M.; Howard, J. A. K.; Marder, T. B.; Stone, F. G. A. *J. Chem. Soc., Chem. Commun.* **1983**, 746. (b) Dawkins, G. M.; Green, M.; Mead, K. A.; Salaun, J. Y.; Stone, F. G. A.; Woodward, P. *J. Chem. Soc., Dalton Trans.* **1983**, 527.

(10) Merola, J. S.; Gentile, R. A.; Ansell, G. B.; Modrick, M. A.; Zentz, S. *Organometallics* **1982**, *1*, 1731.

(11) (a) Martin, B. D.; Matchett, S. A.; Norton, J. R.; Anderson, O. P. *J. Am. Chem. Soc.* **1985**, *105*, 7952. (b) Longato, B.; Martin, B. D.; Norton, J. R.; Anderson, O. P. *Inorg. Chem.* **1985**, *24*, 1389.

Table III. Selected Bond Distances and Angles

		Molecule 1			
		Distances (Å)			
Zr...Mo	3.243 (1)	Mo-P	2.401 (1)	Mo-C1	1.887 (3)
Mo-C2	1.927 (4)	Mo-C21	2.378 (4)	Mo-C22	2.352 (4)
Mo-C23	2.311 (4)	Mo-C24	2.303 (4)	Mo-C25	2.349 (4)
Zr-P	2.647 (1)	Zr-O1	2.290 (2)	Zr-C1	2.344 (3)
Zr-C11	2.515 (3)	Zr-C12	2.500 (3)	Zr-C13	2.507 (3)
Zr-C14	2.514 (3)	Zr-C15	2.536 (3)	Zr-C31	2.518 (3)
Zr-C32	2.518 (3)	Zr-C33	2.500 (3)	Zr-C34	2.491 (3)
Zr-C35	2.506 (3)	O1-C1	1.226 (4)	O2-C2	1.155 (4)
P-C3	1.846 (3)	P-C5	1.851 (3)	C3-C4	1.521 (5)
C5-C6	1.510 (6)				
		Angles (deg)			
C1-Mo-P	98.6 (1)		C2-Mo-P	88.5 (1)	
C2-Mo-C1	90.8 (1)		C1-Zr-P	81.5 (1)	
O1-Zr-P	112.1 (1)		O1-Zr-C1	30.7 (1)	
Zr-P-Mo	79.8 (1)		C3-P-Mo	116.2 (1)	
C3-P-Zr	122.2 (1)		C5-P-Mo	117.9 (1)	
C5-P-Zr	121.3 (1)		C5-P-C3	100.2 (2)	
Zr-C1-Mo	99.5 (1)		O1-C1-Mo	171.1 (2)	
O1-C1-Zr	72.2 (2)		C1-O1-Zr	77.1 (2)	
O2-C2-Mo	176.7 (3)		C4-C3-P	116.5 (3)	
C6-C5-P	113.2 (3)				
		Molecule 2			
		Distances (Å)			
Ti-O1	2.128 (3)	Ti-O4	2.198 (3)	Ti-C21	2.372 (5)
Ti-C22	2.357 (5)	Ti-C23	2.351 (5)	Ti-C24	2.344 (5)
Ti-C25	2.337 (5)	Ti-C31	2.355 (5)	Ti-C32	2.357 (6)
Ti-C33	2.359 (5)	Ti-C34	2.359 (5)	Ti-C35	2.356 (5)
Mo-C1	1.876 (4)	Mo-C2	1.934 (5)	Mo-C3	1.935 (5)
Mo-C11	2.367 (4)	Mo-C12	2.370 (4)	Mo-C13	2.365 (5)
Mo-C14	2.363 (5)	Mo-C15	2.341 (5)	O1-C1	1.205 (5)
O2-C2	1.175 (6)	O3-C3	1.156 (5)	O4-C4	1.456 (5)
O4-C7	1.445 (5)	C4-C5	1.490 (7)	C5-C6	1.465 (8)
C6-C7	1.478 (8)				
		Angles (deg)			
C2-Mo-C1	86.6 (2)		C3-Mo-C1	88.4 (2)	
C3-Mo-C2	91.4 (2)		O4-Ti-O1	78.5 (1)	
C1-O1-Ti	145.0 (3)		C4-O4-Ti	126.3 (3)	
C7-O4-Ti	123.0 (3)		C7-O4-C4	108.3 (3)	
O1-C1-Mo	178.0 (4)		O2-C2-Mo	177.4 (5)	
O3-C3-Mo	176.7 (4)		C5-C4-O4	106.1 (4)	
C6-C5-C4	104.0 (4)		C7-C6-C5	105.1 (4)	
C6-C7-O4	106.3 (4)				

The differing courses of the reactions of the trivalent metallocene phosphides with $[CpMo(CO)_3]_2$ can be attributed to the difference in redox potentials. Generally, reduction potentials for Zr(III)/Zr(IV) redox couples are more negative than the corresponding Ti(III)/Ti(IV) couples. Thus, Ti(III) species are readily formed by reduction of Ti(IV), while Zr(III) is generally much more susceptible to oxidation. These trends are reflected in the present reactions.

Structural Studies. X-ray structural studies of **1** and **2** confirmed the above formulations. Selected interatomic distances and angles for both **1** and **2** are given in Table III. ORTEP drawings of **1** and **2** are shown in Figures 1 and 2, respectively.

For molecule 1, the coordination spheres of the metal atoms can be considered pseudotetrahedral. The M–C distances in the Cp_2Zr and CpMo fragments in **1** are as expected, averaging 2.511 (3) and 2.339 (4) Å, respectively. The bond distances within the terminal carbonyl and PEt_2 fragments are also quite typical and warrant no further comment.

The structural study of **2** confirmed the pseudotetrahedral nature of the Mo and Ti coordination spheres. The Ti–C and Mo–C distances within the Cp_2Ti and CpMo fragments average 2.355 (5) and 2.361 (5) Å, respectively, and are typical, as are the geometries of the cyclopentadienyl rings. Similarly, the geometries of the terminal carbonyl groups on Mo are also as expected. The Ti–O4(THF) distance of 2.198 (3) Å is considerably longer than the Ti–O distances observed for Ti–alkoxide complexes,[13] which is consistent with the relatively poor donor ability of THF. In comparison, the Ti–O1(bridging carbonyl) distance of 2.128 (3) Å is shorter, indicating better donation from the bridging carbonyl group. The O–Ti–O angle of 78.5 (1)° is dramatically smaller than those seen in Ti(IV) dithiolates[3a,b] or Ti(IV) alkoxides.[13] This is consistent with the observations made by Darensbourg et al. for related metallocene d^1 dithiolate species.[3d]

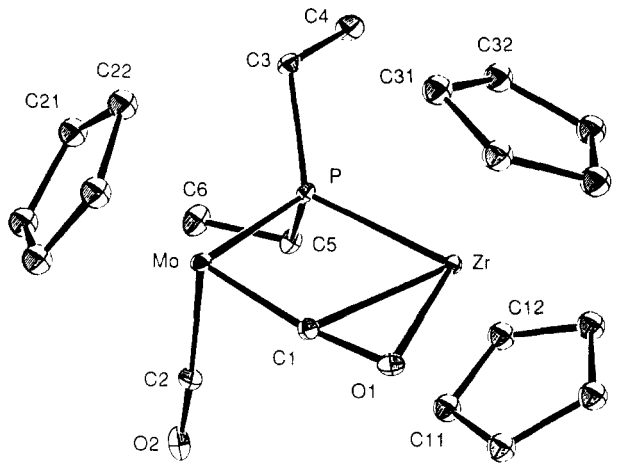

Figure 1. ORTEP drawing of molecule 1. Thermal ellipsoids at the 20% level are shown; hydrogen atoms are omitted for clarity.

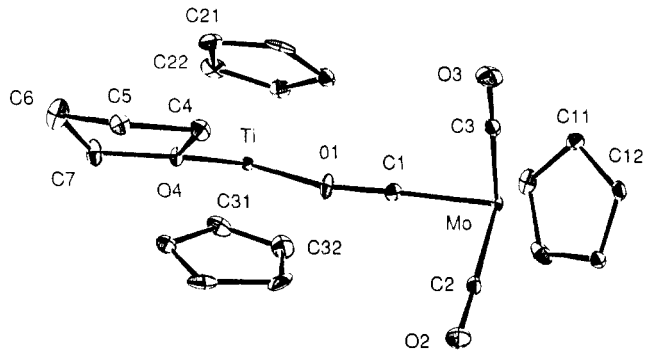

Figure 2. ORTEP drawing of molecule 2. Thermal ellipsoids at the 20% level are shown; hydrogen atoms are omitted for clarity.

The structural details of the core of **1** are presented in Figure 3a. In general, the structure of **1** is very similar to that previously described for $Cp_2Zr(\mu\text{-}PPh_2)(\mu\text{-}\eta^1,\eta^2\text{-}OC)Mo(CO)Cp$.[3c] The Zr–P distance of 2.647 (1) Å and the Mo–P distance of 2.401 (1) Å observed for **1** are significantly shorter than the corresponding distances of 2.704 (1) and 2.417 (1) Å respectively found in $Cp_2Zr(\mu\text{-}PPh_2)(\mu\text{-}\eta^1,\eta^2\text{-}OC)Mo(CO)Cp$. These differences may reflect both the lesser steric demands and the greater basicity of the PEt_2 moiety as compared to that of PPh_2. Similarly, the Zr–P–Mo angle of 79.8 (1)° found for **1** is slightly greater than the corresponding angle of 78.6 (1)° found in the diphenylphosphido-bridged analogue of **1**. The Zr-(η^2-OC) fragment of **1** is remarkably similar to that of $Cp_2Zr(\mu\text{-}PPh_2)(\mu\text{-}\eta^1,\eta^2\text{-}OC)Mo(CO)Cp$. The Zr–O distance in **1** of 2.290 (2) Å compares with that of 2.298 (3) Å found

(12) Gelmini, L.; Matassa, L. C.; Stephan, D. W. *Inorg. Chem.* 1985, *24*, 2585.

(13) (a) Stephan, D. W. *Organometallics*, submitted for publication. (b) Stephan, D. W.; Nadasdi, T. T. Unpublished results. (c) Stephan, D. W.; Toth, R. T. Unpublished results.

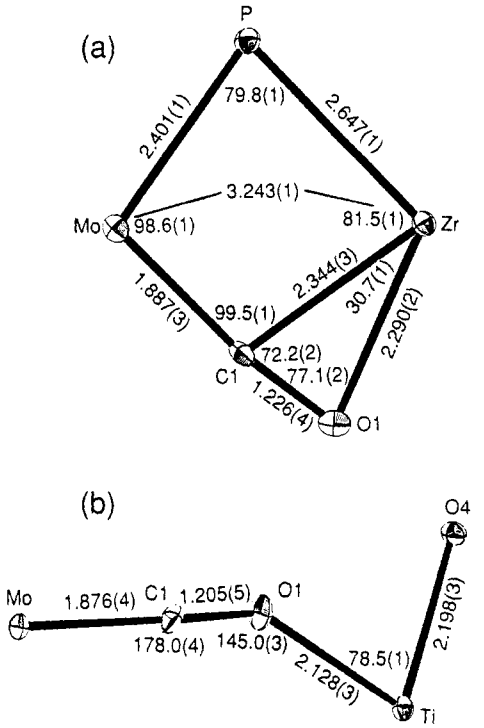

Figure 3. Structural details of the cores of molecules (a) **1** and (b) **2**.

in the diphenylphosphido-bridged analogue. Although this difference is only marginally significant, it is also reflected in the slightly lower carbonyl stretching frequency in **1** (1567 versus 1575 cm^{-1}). Despite this, the C–O bond distances of the η^1,η^2-carbonyl in **1** and $Cp_2Zr(\mu\text{-}PPh_2)(\mu\text{-}\eta^1,\eta^2\text{-}OC)Mo(CO)Cp$ are essentially indistinguishable. Of the known heterobimetallics that contain bridging η^1,η^2-carbonyl groups, only $Cp_2Zr(\mu\text{-}OCMe)(\mu\text{-}\eta^1,\eta^2\text{-}OC)Mo(CO)Cp$[7] exhibits a longer C–O bond (1.241 (1) Å). Thus, the C–O distance of 1.226 (4) Å in **1** is indicative of significant bond order reduction. The Mo–Cl distance of 1.887 (3) Å found for **1** compares with that of 1.876 (4) Å found for $Cp_2Zr(\mu\text{-}PPh_2)(\mu\text{-}\eta^1,\eta^2\text{-}OC)Mo(CO)Cp$ and 1.879 (4) Å for $Cp_2Zr(\mu\text{-}\eta^1,\eta^1\text{-}OC)(\eta^2\text{-}OCMe)Mo(CO)_2Cp$.[11] These data are consistent with back-donation from Mo to the bridging CO.

The Zr–Mo separation of 3.243 (1) Å in **1** is slightly shorter than that observed in $Cp_2Zr(\mu\text{-}PPh_2)(\mu\text{-}\eta^1,\eta^2\text{-}OC)Mo(CO)Cp$ (3.250 (1) Å).[3c] This again may reflect the lesser steric demands of the substituents of the bridging phosphide ligand. These metal–metal separations are substantially longer than in cases where a metal–metal bond has been confirmed. The Zr–Mo distance (3.243 (1) Å) as well as the Zr–P–Mo angle (79.8 (1)°) found in **1** are similar to those found to $Cp_2Zr(\mu\text{-}PPh_2)_2Mo(CO)_4$ (3.299 (1) Å, 79.3 (1)°).[12] These data suggest that metal–metal bonding is weak and support the zwitterionic formulation **1a**, as was previously suggested for $Cp_2Zr(\mu\text{-}PPh_2)(\mu\text{-}\eta^1,\eta^2\text{-}OC)Mo(CO)Cp$.

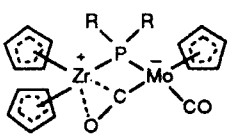

1a

The details of the geometry about the bridging carbonyl moiety are given in Figure 3. The Mo–C–O (bridging carbonyl) angle is essentially linear (178.0 (4)°). The Ti–O–C angle of 145.0 (3)° and the C–O bond distance of 1.205 (5) Å are consistent with substantial C–O bond activation arising from the interaction of the carbonyl with the Lewis acidic Ti center. In comparison to those in other carbonyl-bridged Ti/Mo complexes (Table IV), the C–O distance observed in **2** is relatively short. The C–O distance is comparable to that found in the one other structurally characterized Ti(III)/Mo complex, $[Cp_2Ti(\mu\text{-}OC)Mo(CO)_2(C_5H_4Me)]_2$.[14] A marginally longer C–O bond distance and lower C–O stretching frequency are observed for the Ti(IV)/Mo species $Cp^*_2(Me)Ti(\mu\text{-}\eta^1,\eta^1\text{-}OC)Mo(CO)_2Cp$.[15] A substantially longer bridging C–O distance is reported for $[Cp^*_2Ti(\mu\text{-}OC)Mo(CO)Cp]_2$, where the carbonyl bound to Ti also bridges the two Mo centers.[16] Thus, the activation is enhanced by both back-donation from the two Mo centers and the interaction with the Lewis acidic Ti(III) center.

The present results indicate that several features affect the degree of C–O bond activation by a heterobimetallic complex. The nature of the CO–early-metal interaction clearly has an effect. In a comparison of the bridging CO

Table IV. Structural and Spectroscopic Data for Carbonyl-Bridged Ti/Mo Complexes[a]

compd	μ-C–O, Å	ν_{CO}, cm^{-1}	ref
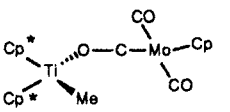	1.212 (5)	1627	15
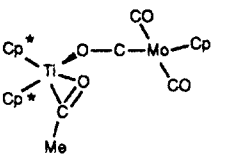		1700	17
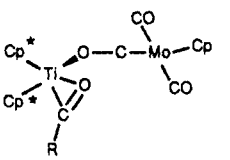 R = neopentyl		1700	17
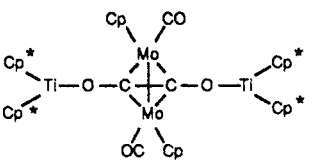	1.271 (7)	1351	16
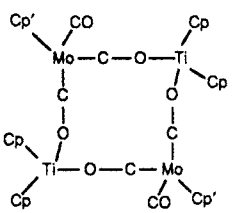	1.208 (7)	1710	14
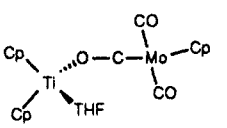	1.205 (5)	1657	this work, 10

[a] The structural and spectral data given refer to the bridging carbonyl moieties.

(14) Merola, J. S.; Campo, K. S.; Gentile, R. A.; Modrick, M. A.; Zentz, S. *Organometallics* **1984**, *3*, 334.
(15) Hamilton, D. M.; Willis, W. S.; Stucky, G. D. *J. Am. Chem. Soc.* **1981**, *103*, 4255.
(16) De Boer, E. J. M.; De With, J.; Orpen, A. G. *J. Chem. Soc., Chem. Commun.* **1985**, 1666.

moieties of 1 and 2, it seems that interaction of the early metal with the C-O π cloud results in greater bond order reduction than does donation from a lone pair of electrons on oxygen to a Lewis acidic center. Of course, another factor in the comparison of 1 and 2 is the Lewis acidity of the early-metal center. Comparison of the complexes $Cp_2Zr(Me))(\mu\text{-}\eta^1,\eta^1\text{-}OC)Mo(CO)_2Cp$(C-O 1.236 (5) Å, 1545 cm^{-1})[17] and $Cp^*_2Ti(Me)(\mu\text{-}\eta^1,\eta^1\text{-}OC)Mo(CO)_2Cp$(C-O 1.212 (5) Å, 1623 cm^{-1})[15] suggests that Zr(IV) is a more effective Lewis acid than Ti(IV). Thus, it appears both the nature of the CO-metal interaction and the Lewis acidity of the early metal favor C-O bond activation in 1 relative to that in 2.

Acknowledgment. Financial support from the NSERC of Canada is gratefully acknowledged. D.G.D. is grateful for the award of an NSERC of Canada postgraduate scholarship.

Supplementary Material Available: Tables of thermal and hydrogen atom positional parameters and bond distances and angles associated with the cyclopentadienyl rings (6 pages); a listing of values of $10F_o$ and $10F_c$ (18 pages). Ordering information is given on any current masthead page.

(17) De Boer, E. J. M.; De With, J. *J. Organomet. Chem.* **1987**, *320*, 289.

Organometallic Oxides: Preparation, Structure, and Chemical and Physical Properties of Paramagnetic $[(\eta\text{-}C_5H_5)NbCl(\mu\text{-}A)]_3(\mu_3\text{-}OH)(\mu_3\text{-}O)$ (A = Cl, OH) and Other Oxo-Hydroxo Clusters of Niobium†

Frank Bottomley,* Petra N. Keizer, and Peter S. White

Department of Chemistry, University of New Brunswick, Fredericton, New Brunswick, Canada E3B 5A3

Keith F. Preston

Division of Chemistry, National Research Council of Canada, Ottawa, Ontario, Canada K1A 0R9

Received January 17, 1990

Hydrolysis of $Cp'NbCl_4$ ($Cp' = \eta^5\text{-}C_5H_5$ (Cp), $\eta\text{-}C_5H_4Me$ (Cp^1)) in tetrahydrofuran (THF) gave a mixture of products of general formula $[Cp'NbL_4]_2(\mu\text{-}O)$, where L_4 is a combination of H_2O and terminal or bridging Cl that gives eight-coordinate, pentavalent, niobium. For Cp' = Cp, a major constituent of the mixture is $[CpNb(H_2O)Cl_3]_2(\mu\text{-}O)\cdot 2THF\cdot 0.5Et_2O$ (1), the structure of which was determined by X-ray diffraction. Crystal data: monoclinic; $C2/c$; a = 22.105 (4) Å, b = 11.366 (1) Å, c = 15.563 (2) Å, β = 124.71 (1)°; R = 0.056 for 165 parameters and 1444 observed $|F_o|$. The Nb-O-Nb angle in 1 is 173.7 (7)°, and the torsion angle between the $[CpNb(H_2O)Cl_3]$ units is 78.8 (3)°. The H_2O ligands are hydrogen-bonded to lattice THF. Reduction of $[Cp'NbL_4]_2(\mu\text{-}O)$ with aluminum powder gave the cluster $[Cp'NbCl(\mu\text{-}Cl)]_3(\mu_3\text{-}OH)(\mu_3\text{-}O)$ (2). The structure of 2 (Cp' = Cp) as the THF adduct was determined by X-ray diffraction. Crystal data: monoclinic; $P2_1/c$; a = 9.966 (1) Å, b = 12.471 (2) Å, c = 20.321 (2) Å, β = 93.86 (1)°; R = 0.027 for 307 parameters and 3507 observed $|F_o|$. 2 has an isosceles triangle of CpNbCl groups (Nb-Nb = 2.823 (1), 3.239 (1), 3.252 (1) Å) with edge-bridging Cl and face-bridging OH and O ligands. The OH is hydrogen-bonded to the lattice THF. The Nb-Nb distances indicate a single Nb-Nb bond between Nb(1) and Nb(2) but no interaction between Nb(1) or Nb(2) and Nb(3). This model is borne out by the magnetic moment of 2, 1.39 μ_B (295 K), and by the ESR spectrum. The g and ^{93}Nb hyperfine interaction tensors, derived from a spectral analysis of 2, are parallel and axial within experimental error ($g_\parallel$ = 1.9232, $g_\perp$ = 1.9832; $a_\parallel^{93}$ = 649 MHz, $a_\perp^{93}$ = 303 MHz) and show that the unpaired electron is located on Nb(3) in a d_{xy} orbital that makes an angle of approximately 45° to the Nb_3 plane. There is no coupling to the other Nb nuclei or to Cl. Extended Hückel calculations confirm this assignment. The ESR spectrum also shows that 2 exists as two isomers with the proton attached to an oxygen atom either above or below the plane of the Nb atoms. $[Cp'NbCl(\mu\text{-}Cl)]_3(\mu_3\text{-}OH)(\mu_3\text{-}O)$ decomposed slowly in THF solution to give a species formulated as $Cp'_4Nb_5Cl_5(OH)_9O(THF)_2$ (5) on the basis of spectroscopy, analysis, and a partial structure determination; 5 has an adamantane-like $Nb_4(OH)_6$ core and a magnetic moment of 1.86 μ_B. Reduction of $[CpNbL_4]_2(\mu\text{-}O)$ with zinc powder gave units of $[CpNbCl(\mu\text{-}OH)]_3(\mu_3\text{-}OH)(\mu_3\text{-}O)$ (3) connected by ZnCl(OH)(THF). Spectroscopic and magnetic methods establish that 3 has a structure similar to that of 2, with edge-bridging OH instead of Cl.

Introduction

We are synthesizing cyclopentadienylmetal oxides that retain the properties of conventional metal oxides but are soluble in nonpolar solvents. Three general routes to such oxides may be envisaged. The first is oxidation of a cyclopentadienylmetal complex by a source of oxygen. The second is treatment of a metal oxide with a cyclopentadienyl salt. The third is to aggregate a mononuclear or low polynuclear cyclopentadienylmetal oxo complex. We have had considerable success with the first method, obtaining clusters such as $Cp_{14}V_{16}O_{24}$,[1] $[CpV]_5(\mu_3\text{-}O)_6$,[2,3] and

† Issued as NRC No. 31257.

(1) Bottomley, F.; Paez, D. E.; White, P. S. *J. Am. Chem. Soc.* **1985**, *107*, 7226.

0276-7333/90/2309-1916$02.50/0